Recurrence of Drought Events Over Iberia. Part II: Future Changes Using Regional Climate Projections

JULIA MOEMKEN [iD]

BENJAMIN KOERNER

FLORIAN EHMELE [iD]

HENDRIK FELDMANN [iD]

JOAQUIM G. PINTO [iD]

*Author affiliations can be found in the back matter of this article

STOCKHOLM
UNIVERSITY PRESS

ABSTRACT

Seasonal droughts are a common feature of the Iberian (Mediterranean) climate. They can have severe impacts on both natural and human life – especially, when recurring in consecutive years. In this study, we investigate the potential impacts of climate change on recurrent drought events in the Iberian Peninsula (IP). With this aim, we use the new set of indices introduced in Moemken and Pinto (2022): the Recurrent Dry Year Index (RDYI) and the Consecutive Drought Year (CDY) Index. These are applied to a large EURO-CORDEX multi-model ensemble consisting of 25 different global-to-regional model (GCM-RCM) chains that follow the RCP8.5 scenario with 12 km horizontal resolution. A drizzle correction and a simple multiplicative approach are used to bias-adjust the daily precipitation sums.

Results reveal a general tendency towards more severe drought conditions in IP under different global warming levels (GWLs). Moreover, recurrent drought events are projected to occur more frequent and last longer. While the ensemble mean responses are only moderate for a GWL of +2°C (compared to the pre-industrial average), recurrent drought conditions are strongly enhanced for the +3°C GWL. The magnitude of projected changes shows some sensitivity on the choice of index and model. Typically, changes are more pronounced for indices based on the effective drought index (EDI) and show a larger spread for the individual GCMs than for the various RCMs. Nevertheless, the climate change signals are robust for most of IP and all indices, with a larger model agreement for the +3°C GWL. We conclude that the Iberian Peninsula is confronted with an increased risk of recurrent drought events in future decades. If global warming should exceed the +3°C threshold, the majority of models projects an almost permanent state of drought – which could result in severe implications for the Iberian population and ecosystems.

CORRESPONDING AUTHOR:

Julia Moemken

Karlsruhe Institute of Technology (KIT), Institute of Meteorology and Climate Research, Wolfgang-Gaede-Str. 1, 76131 Karlsruhe, DE

julia.moemken@kit.edu

1. INTRODUCTION

Given ongoing climate change and population growth, the world is confronted by an increasing number of complex challenges – including the high-risk impacts of extreme weather and climate events (World Economic Forum, 2019). Among these extremes, droughts are one of the most impacting, yet least understood disasters (Wilhite et al., 2007; Spinoni et al., 2018). One reason is the complex interplay of atmospheric, biogeophysical and hydrological processes that leads to drought development (Touma et al., 2015). Consequently, there is no unique but rather a wide variety of definitions and indicators used to identify and characterize droughts (WMO, 2006; Mishra and Singh, 2010; Dai, 2011). This, in turn, results in large uncertainties regarding worldwide drought trends under present and future climate conditions (Dai, 2011; Sheffield et al., 2012; Trenberth et al., 2014; Tramblay et al., 2020).

One region displaying rather consistent trends is the Mediterranean, Europe's drought hotspot (Hoerling et al., 2012; Spinoni et al., 2015a; b). In particular, the Iberian Peninsula (IP) has suffered from an increase in drought frequency and intensity in the last decades (Coll et al., 2017; Páscoa et al., 2017; Spinoni et al., 2017). As a result, the risk of water scarcity in the region is likewise increasing, as water demand is already close to water availability under normal conditions (e.g. Iglesias et al., 2009). Thereby, droughts critically affect various water using sectors in IP, from agriculture over economy to society (Ciais et al., 2005; Blauhut et al., 2015; Naumann et al., 2015; Haberstroh et al., 2021).

In the context of climate change and global warming, the risk and impacts of extreme events in Europe is projected to increase (Seneviratne et al., 2012; Forzieri et al., 2016; IPCC, 2021). In particular, the impact of drought could be aggravated in future decades (Hirschi et al., 2011; Dai, 2013; Seneviratne et al., 2013). Moreover, droughts are projected to develop faster, be longer-lasting and more severe (e.g. Cook et al., 2015). For the 21st century, climate projections indicate a decrease in mean precipitation and a simultaneous increase in the frequency and intensity of drought events for IP (Seneviratne et al., 2012; Stagge et al., 2015; Santos et al., 2016; Spinoni et al., 2018; 2020). This may result in shorter return periods of extreme drought events in future decades (e.g. Barriopedro et al., 2011). At the same time, an enhanced year-to-year variability of precipitation is projected, which may lead to an increased occurrence of multiple drought events in a single decade, even in consecutive years. A careful regional assessment of such recurrent drought events is critical since these temporal compounding events typically exacerbate the impacts (Zscheischler et al., 2020). Additionally, even small variations in magnitude and frequency of recurrent events can have huge effects, especially on semi-arid ecosystems.

For the first time, we explicitly focus on the recurrence of dry/drought events in consecutive years in IP under future climate conditions. Thereby, we want to answer the following research questions:

- How will recurrent dry/drought events in IP change with ongoing climate change? More precisely, will these events become longer and/or more frequent?
- Are the climate change signals consistent among regional climate projections and different indices?

With this aim, we build on the preceding study by Moemken and Pinto (2022) and utilize the newly introduced set of indices: the Recurrent Dry Year Index (RDYI) and the Consecutive Drought Year (CDY) Index. As input data, our study uses high-resolution regional climate simulations provided by EURO-CORDEX (European domain of the Coordinated Regional climate Downscaling Experiment; Giorgi et al., 2009) with a resolution of 0.11° (approx. 12 km). In total, the multi-model ensemble consists of 25 global-to-regional climate model (GCM-RCM) chains. Since models show systematic biases and e.g. have difficulties reproducing observed rainfall distributions (e.g. Feldmann et al., 2008; Berg et al., 2012; Ehmele et al., 2020), daily precipitation sums are bias-adjusted by applying a simple multiplicative approach (Berg et al., 2012). Furthermore, the bias adjustment ensures the comparability between the different GCM-RCM chains. We derive ensemble statistics and (recurrent) drought characteristics for two global warming levels (GWLs): +2°C and +3°C above pre-industrial average. Results are compared to a historical reference period (1971–2000), which corresponds to a +0.5°C global warming (Teichmann et al., 2018). We evaluate the climate change scenario RCP8.5 (Meinshausen et al., 2011) of the EURO-CORDEX ensemble to identify possible changes in the maximum duration and frequency of recurrent drought events in future decades.

The manuscript is organized as follows: Chapter 2 describes the region of interest (2.1), the datasets (2.2), the used bias adjustment (2.3), and the applied drought indices (2.4). Chapter 3 focuses on the results, while Chapter 4 concludes this paper with a summary and discussion of results.

2. STUDY AREA, DATA AND METHODS

2.1 STUDY AREA

The Mediterranean region lies in the transition zone between the moderate Central European mid-latitude climate and the subtropical desert zones of North Africa. Its main climatic characteristics are mild/humid winters and hot/dry summers (e.g. Maheras et al., 1999;

Hertig, 2004). The precipitation regime of IP (and the Western Mediterranean in general) is characterized by a pronounced seasonality, strong variability on inter-annual and decadal time scales as well as large regional variations (e.g. Esteban-Parra et al., 1998; Rodriguez-Puebla et al., 1998). The rainiest part is the Northwest IP (*Figure 1*), which is strongly influenced by Atlantic low-pressure systems, especially during winter. The driest regions are found in Central IP and along the south-eastern coast. Throughout the year, highest precipitation amounts typically occur during winter (October to March), while nearly every summer features a seasonal drought (Esteban-Parra et al., 1998; Rodriguez-Puebla et al., 1998; Trigo et al., 2004; Paredes et al., 2006). Thus, the major drought events in IP are usually triggered by a lack of precipitation during the winter half year (Trigo and DaCamara, 2000; Caldeira et al., 2015).

Our study focuses on the IP (red box in *Figure 1a*) as defined in the PRUDENCE regions by Christensen and Christensen (2007), namely 10°W-3°E and 36°N-44°N. Some analyses are exemplarily done for five Iberian sub-regions (*Figure 1b*): the Northwestern (IP-NW; 10°W-5°W, 40°N-44°N), the Northeastern (IP-NE; 5°W-0°E, 40°N-44°N), the Southwestern (IP-SW; 10°W-5°W, 36°N-40°N), the Southeastern (IP-SE; 5°W-0°E, 36°N-40°N), and the Eastern area (IP-E; 0°E-3°E, 38°N-44°N). We consider only grid points over land for our analysis.

2.2 DATA

We investigate recurrent drought events in a large multi-model ensemble, simulated within the framework of EURO-CORDEX (Giorgi et al., 2009; Jacob et al., 2014). It comprises 25 GCM-RCM chains, resulting from 5 RCMs each driven by the same 5 GCMs (see *Table 1*). We chose this particular ensemble to account for model uncertainties and increase the robustness of results. Additionally, such a big ensemble enables the investigation of the influence of different GCMs and RCMs. The data have a spatial resolution of 0.11° (~12 km) and the model output is analysed at daily temporal resolution.

We analyse climate change information for different global warming levels (GWLs). These indicate changes in global surface temperature relative to pre-industrial climate conditions. For many variables, regional climate impacts relate quasi-linearly to changes in global mean temperature and are often consistent across different emission scenarios for a given GWL (IPCC, 2021). In our study, we focus on the +2°C and +3°C GWLs with respect to the pre-industrial period 1881–1910. We use the time sampling approach following Vautard et al. (2014) and Teichmann et al. (2018) to identify the climate change signals that are associated with the respective GWL. Accordingly, for each of the 5 GCMs in the ensemble, the 30-year period is determined in which the global temperature increases on average by +2K (+3K) relative to pre-industrial levels (see *Table 2*). The corresponding
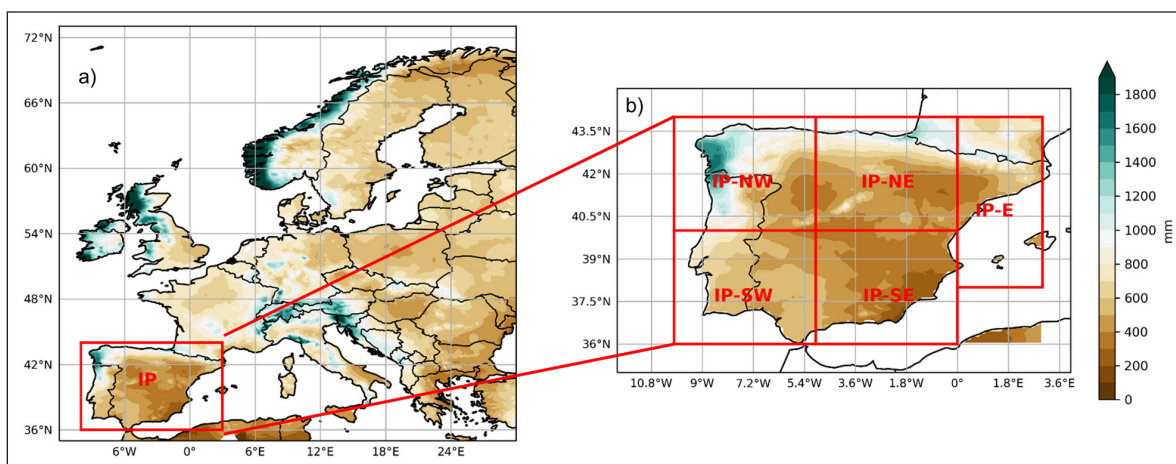
Figure 1 Climatology of annual precipitation (mm) for 1971–2000 derived from E-OBS. (**a**) Europe, with Iberian Peninsula as defined by Christensen and Christensen (2007) marked by red box; (**b**) Iberian Peninsula with sub-regions as used in this study.

GCM	RCM
CNRM-CM5 (Voldoire et al., 2013)	COSMO-CLM4-8-17 (Rockel et al., 2008)
EC-EARTH (Prodhomme et al., 2016)	HIRHAM5 (Christensen et al., 1998)
HadGEM2-ES (Collins et al., 2011)	RACMO22E (Meijgaard et al., 2012)
MPI-ESM-LR (Giorgetta et al., 2013)	RCA4 (Samuelsson et al., 2011)
NorESM1-M (Bentsen et al., 2013)	REMO2015 (Jacob et al., 2012)

Table 1 Overview on GCM-RCM model chains (including references) used in this study. Every RCM is driven with every GCM.

GCM	+2°C PERIOD	+3°C PERIOD
CNRM-CM5	2029 – 2058	2052 – 2081
EC-EARTH	2026 – 2055	2051 – 2080
HadGEM2-ES	2016 – 2045	2037 – 2066
MPI-ESM-LR	2029 – 2058	2052 – 2081
NorESM1-M	2031 – 2060	2057 – 2086

Table 2 30-year periods under which the GCMs show a global warming level (GWL) of +2°C and +3°C.

warming of the historical reference period 1971–2000 results from the observed mean global temperature increase compared to the middle of the period 1881–1910 and corresponds to +0.5K. Please note that the +2°C GWL (+3°C GWL) thus corresponds to a warming of +1.5°C (+2.5°C) from 1971–2000 to the +2°C (+3°C) period. This has to be considered when interpreting the results. The future climate projections were carried out under the RCP8.5 scenario (Meinshausen et al., 2011). This scenario represents a high-emission, non-mitigation scenario and corresponds to 8.5 W/m² anthropogenic radiative forcing by 2100, leading to a global temperature increase of around 3–4°C by the end of the century. While it was created as a worst-case scenario, RCP8.5 is currently closest to the actual observed emissions (Peters et al., 2013; Friedlingstein et al., 2019; Schwalm et al., 2020). We have chosen this scenario for its large data availability and to ensure that the +3°C GWL is reached in all simulations.

Following the IPCC definition and Jacob et al. (2014), we use the model consistency/congruence to assess the robustness and uncertainty of climate change signals. Accordingly, trends are defined as robust/likely (or not) if more (less) than 68% of the ensemble members agree on the sign of change – in this study, this corresponds to 17 out of 25 members.

To validate the historical model simulations, daily precipitation sums were obtained from the ensemble version of E-OBS: V20e (Haylock et al., 2008; Cornes et al., 2018) with a resolution of 0.1°. The accuracy of E-OBS depends strongly on the station coverage over Europe and is therefore rather heterogeneous (Cornes et al., 2018). Nevertheless, E-OBS is widely used for model evaluation studies (e.g. Min et al., 2013; Herrera et al., 2016) and bias adjustment (e.g. Cardell et al., 2019).

2.3 BIAS ADJUSTMENT

Climate models on both global and regional scales tend to show systematic biases, typically associated with an incorrect representation of physical processes, flaws in the model structure or errors in the initialisation (e.g. Liang et al, 2008; Ehret et al., 2012). In terms of precipitation, the model biases may, for example, lead to inaccurate rainfall distributions or a biased annual cycle (e.g. Feldmann et al., 2008; Berg et al., 2012; Ehmele

et al., 2020; 2022). This could in the following result in an under- or overestimation in the number of drought events. Therefore, a bias adjustment is applied before identifying droughts in the model data and calculating ensemble statistics. Moreover, the bias adjustment enhances the comparability of the various GCM-RCM chains.

A detailed overview on available bias correction methods for precipitation is given, for example, in Fang et al. (2015) and Maraun (2016). For our study, it is crucial that the annual cycle and the spatial distribution of precipitation in IP are realistically represented by all ensemble members. This is already achievable with simple linear methods. In contrast, the often used distribution-based methods, such as quantile mapping (e.g. Yang et al., 2018; Cardell et al., 2019; Ehmele et al., 2022), have problems with the adjustment in the dry summer months (Iberian summer drought), when only few to no precipitation events can be used for the calculation. Thus, we applied a 'simple multiplicative correction' (Berg et al., 2012), which scales the precipitation data to correct the monthly mean bias. This approach, like any other, assumes that the bias between observations and models is stationary and does not change under future climate conditions. First, a drizzle correction, which removes all precipitation values below 0.1 mm/day, is employed. These values, although being potentially numerical correct, are physically not relevant. In the next step, the ratio of the mean monthly precipitation sums of E-OBS and the EURO-CORDEX data is calculated for the reference period (1971–2000). This 'correction factor' is calculated separately for each grid point and each of the 25 EURO-CORDEX simulations. It is then used to scale the model data for all daily time steps d in month m and at every grid point:

$$pr_{corr}^m(d) = pr_{mod}^m(d) * \frac{\overline{pr_{obs}^m}}{\overline{pr_{mod}^m}}$$

Where pr_{corr}^m is the corrected precipitation, pr_{mod}^m is the raw model output, and $\overline{pr_{obs}^m}$ and $\overline{pr_{mod}^m}$ are the mean monthly sums of observations and models, respectively. Please note that correction factors below 0.02 (above 50) are possible mainly due to the heterogeneity of the observations and are therefore set to 0.02 (50) to prevent unrealistic values. The estimated 'correction factors' are then used to adjust the future projections.

Figure S1a (Supporting Information) shows the bias in the ensemble mean for the uncorrected (raw) EURO-CORDEX data, depicted as the ratio in mean annual precipitation between the EURO-CORDEX ensemble and E-OBS. In general, the raw model data overestimates annual precipitation for almost all of IP. In some regions, such as Central IP, modelled precipitation is more than twice as high as the observed one. Moreover, some individual ensemble members differ considerably from

each other and from E-OBS (Figure S1b). After applying our bias correction approach, the bias in spatial annual rainfall distribution is clearly reduced (Figure S1c), lying now within the 5% range. Moreover, the characteristics of the chosen bias correction method also enabled the adjustment of the annual cycle of precipitation for all GWLs in all ensemble members (Figure S2).

Based on the above results, we conclude that the chosen bias adjustment method performs sufficiently well to assess the research questions of this study. Nevertheless, care has to be taken as the quality of the bias correction strongly depends on the quality and availability of the observations.

2.4 DROUGHT INDICES

A set of indices is employed to identify and investigate both single and recurrent meteorological drought events over IP. The input for all indices is precipitation and/or its deviations from the long-term climatological mean. We use the historical period 1971–2000 (corresponding to a global warming level of +0.5°C) as climatological reference for the calculation of both historical and future drought indices, thus considering explicitly the climate change signal. All analyses focus on the hydrological year (1st October to 30th September). In the following, we always refer to the hydrological year when using terms like annual, yearly, or year.

For *single drought events*, we apply the following two indices: The one-dimensional drought index (DI) uses the precipitation deficit and the affected area as measures (Moemken and Pinto, 2022). Thus, a drought year is identified if the following criteria are fulfilled at the same time:

- Annual precipitation amount is below 65% of the climatological mean, and
- At least 10% of all grid points in IP are affected by this precipitation deficit.

The second index is the Effective Drought Index (EDI), which was developed by Byun and Wilhite (1999). Previous studies used this index to assess drought characteristics for various regions around the world under present (Khodayar et al. (2015) for Europe; Lee et al. (2015) for South Korea; Deo et al. (2017) for Australia) and future climate conditions (Kim and Byun (2009) for Asia; Kamruzzaman et al. (2019) for Bangladesh). EDI is based on the calculation of the effective precipitation that considers the precipitation accumulation of the last 365 days at any given time and at every single grid point with a weighting function, thereby simulating the loss/gain of soil moisture over time. It is a centred, symmetric, and standardized index, which is worldwide applicable. We use the following categories to classify dry/drought periods (cf. Khodayar et al., 2015):

- Normal: $1.0 > EDI > -1.0$
- Dry: $-1.0 \geq EDI > -1.5$
- Severe dry: $-1.5 \geq EDI > -2.0$
- Extreme dry: $EDI \leq -2.0$

As proposed by Moemken and Pinto (2022), a drought year is identified if EDI is below –1.0 on at least 90 days of the year, which do not need to be consecutive.

For *recurrent dry/drought events*, we employ the new indices introduced and validated for the current climate by Moemken and Pinto (2022). These are based on the concept of Consecutive Dry Days (CDD), which was developed by the "Expert Team of Climate Change Detection Indices" (ETCCDI; van Engelen et al. 2008; Zhang et al., 2011). The new indices quantify either the maximum duration of recurrent events or their frequency. To be classified as recurrent, these events must comprise at least two consecutive dry/drought years.

The first index is the Recurrent Dry Year Index (RDYI). It counts the maximum number of consecutive dry years within a certain time period (in this study 30 years) at every single grid point. A year is defined as a dry year when the annual precipitation amount is below 65% of the climatological mean. A series of at least two consecutive dry years (RDYI ≥ 2) is called a dry year period. The corresponding frequency index NDYP estimates the number of dry year periods within the considered time period (here 30 years).

The second index is the Consecutive Drought Year Index (CDY and CDY-EDI). Similar to RDYI, it counts the maximum number of consecutive drought years, but this time based on DI or EDI. Additionally, the Number of Drought Periods (NDP and NDP-EDI) with CDY (or CDY-EDI) ≥ 2 is computed. Due to the definition of DI, CDY (NDP) is a one-dimensional index with a single value for each sub-region or whole IP, while CDY-EDI (NDP-EDI) is calculated at every grid point and spatially averaged later on for comparison.

Please note that both the maximum duration and the frequency depend on the timing of normal/wet years in a 30-year-time series for recurrent events persisting longer than 10 years. The date of these 'non-drought' years determine whether recurrent events are longer and less frequent or shorter and more frequent. Thus, the two characteristics of recurrent events should always be considered and interpreted together.

3. RESULTS
3.1 FUTURE CHANGES IN DROUGHT CHARACTERISTICS
3.1.1 Drought indices
In a first step, we analyse potential future changes for single drought events. With this aim, we focus on changes in the mean and variability of EDI. The changes

of mean EDI are presented in *Figure 2* for the ensemble mean projections for a global warming of +2°C and +3°C, respectively. Areas showing robust signals, meaning that at least 68% of the ensemble members agree on the sign of change (see also Section 2.2), are dotted. Spatially averaged signals of the individual ensemble members are shown in Supplementary Figures S3 and S4, respectively. In these figures, the separate boxes of each matrix represent the value of the individual GCM-RCM model chains for the whole IP. RCMs (GCMs) are arranged in rows (columns), and the corresponding RCM mean (GCM mean) is given in the first column (last row). For the +2°C GWL, the ensemble mean projects a drying for most of IP, with 18 out of 25 ensemble members agreeing on the signal (Figure S3f). Strongest trends are found for mountain ranges (e.g. Cantabria) and large parts of Portugal, with EDI values around −0.4 (corresponding to −0.4 standard deviations compared to the historical reference period). Slightly positive, though non-robust trends are found along the eastern Mediterranean coast. In general, weakest (strongest) signals can be found for simulations driven with CNRM-CM5 (MPI-ESM-LR). Climate change signals increase in magnitude and robustness for a GWL of +3°C (*Figure 2b*). Negative EDI changes and thus a drying trend is simulated for all of IP by 24 of the

25 ensemble members (Figure S4f). Nevertheless, the ensemble spread is higher than for the +2°C GWL. On average, values are in the range of −0.2 to −0.6, but may locally reach up to −0.8. Signals are again lowest for CNRM-CM5-driven runs, while strongest trends are obtained for simulations with MPI-ESM-LR and NorESM1-M. While the ensemble mean EDI trends are quite similar in all sub-regions and periods (Figures S3 and S4), the individual ensemble members do show different regional drying trends, which are primarily driven by the choice of GCM. Most of the ensemble members agree on weakest trends for IP-E and largest drying trends for IP-SE and IP-SW.

Changes in the temporal variability of EDI are depicted in *Figure 3* for the ensemble mean and both future GWLs. An overview of the climate signals of the individual ensemble members is given in Figures S5 and S6. The variability is calculated as standard deviation of daily EDI values. For the +2°C GWL, the ensemble mean simulates a higher temporal variability compared to the historical period, especially for the northern inland and along the eastern Mediterranean coast. This increase in variability is likely/robust for most of IP as all ensemble members agree on the trend (Figure S5f). For the +3°C GWL, the ensemble mean reveals a larger ensemble spread and a North–South gradient in variability trends. Most ensemble
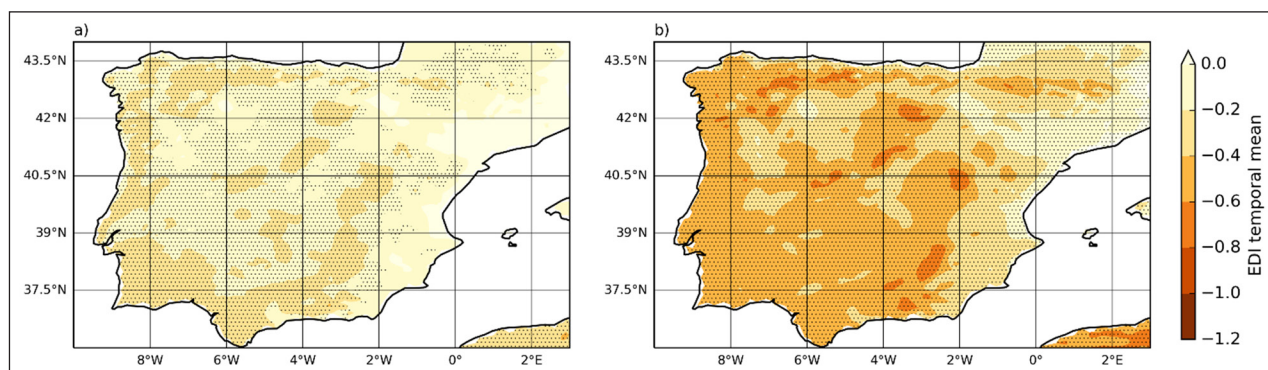
Figure 2 Changes in effective drought index (EDI) for the multi-model ensemble mean for a global warming level (GWL) of (**a**) +2°C, and (**b**) +3°C relative to the pre-industrial level. Reference is the historical period 1971-2000 (corresponds to a GWL of +0.5°C). Black dots indicate robust climate change signals, meaning that 17 or more ensemble members (corresponds to 68%) agree on the sign of change.
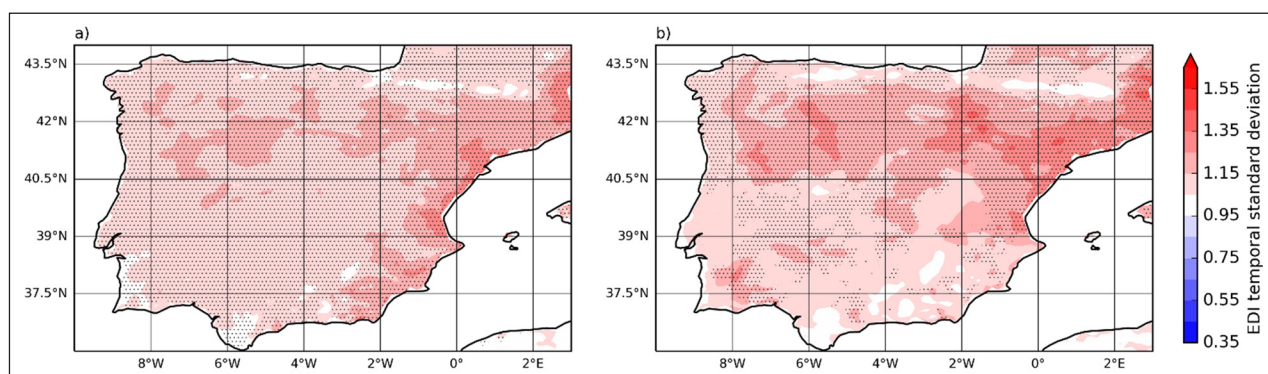
Figure 3 Changes in EDI variability for the multi-model ensemble mean for a GWL of (**a**) +2°C, and (**b**) +3°C. Reference is the historical period 1971–2000 (corresponds to a GWL of +0.5°C). Black dots indicate robust climate change signals, meaning that 17 or more ensemble members (corresponds to 68%) agree on the sign of change.

members project an increase in variability for Northern IP. For Southern IP, some runs driven by HadGEM2-ES and NorESM1-M project a decrease in variability (attributed to the near-constant drought conditions; see also Section 3.2), while all other simulations agree on a stationary or increasing variability in this region (Figure S6).

Overall, we see a clear shift towards drier conditions and thus drought occurrence in IP with increasing levels of global warming. The projected trends are robust for most of IP under a +2°C GWL and for all of IP for the +3°C GWL. Differences between individual ensemble members are mainly determined by the selection of the driving GCMs, as the difference between RCMs for the same GCM are comparatively small.

3.1.2 Processes influencing drought events

To illustrate the potential causes for this increase in drought occurrence, **Figure 4** displays the annual cycle of several key parameters and their changes, derived from the ensemble mean averaged over the IP domain for the reference period and the two GWLs. The temperature changes (**Figure 4a**) are relatively constant over the year and do not deviate strongly from the respective warming levels. The maximum precipitation occurs in winter and to a lesser degree in spring (**Figure 4b**). In summer (JJAS) there is a distinct dry season. The ensemble displays a slight increase of monthly precipitation of up to ~5% from January to March for the +2°C GWL and from February to March for the +3°C GWL. Strongly reduced precipitation rates are found for the rest of the year, especially from May to October. The reduction of the monthly amounts is more pronounced with up to 25% for the +3°C GWL than for the +2°C level, where the reduction reaches about 13%. Overall, the simulations indicate a net reduction of the annual precipitation amounts by 6% in a 2°C and by 13% in a 3°C warmer world.

The soil moisture (**Figure 4c**) has its maximum in late winter/early spring and its minimum in August/September. The absolute changes are fairly constant over the year. However, the relative changes represent a slightly lesser reduction in spring and a stronger reduction in the dry summer and autumn (up to –5% for the +2° C GWL and about –7.5% for the +3°C GWL).
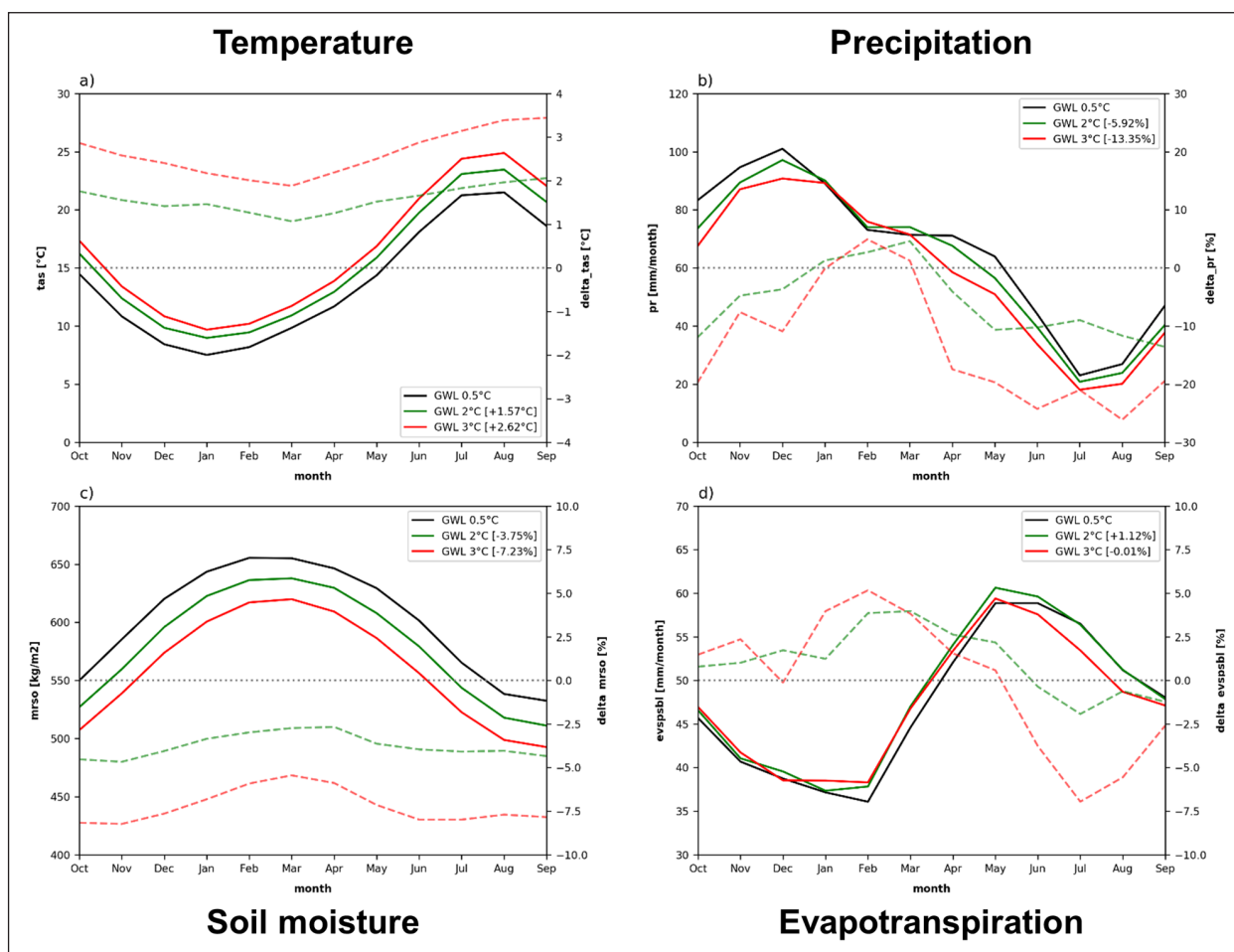
Figure 4 Mean annual cycle (solid lines) of monthly (**a**) temperature (tas; °C), (**b**) precipitation (pr; mm/month), (**c**) soil moisture (mrso; kg/m²), and (**d**) evapotranspiration (evspsbl; mm/month) – for a GWL of +0.5°C (black), +2°C (green), and +3°C (red). Climate change signals (dashed lines; °C for tas and % for the rest) calculated as GWL2°C – GWL0.5°C (green) and GWL3°C – GWL0.5°C (red). The values in brackets indicate the mean annual change. Depicted is the multi-model ensemble mean, spatially averaged for IP. Please note that we use direct model output.

The highest evapotranspiration (*Figure 4d*) occurs in spring at the end of the rainy period with rising temperatures and insolation. From summer to winter the amounts of evaporation decrease. The future changes are expected to generate a slight increase from October to May due to the increased temperatures and partly due to the slightly increased precipitation amounts. From June to September the evapotranspiration decreases slightly (up to –2%) for the +2°C GWL and more pronounced (up to –7.5%) for the +3°C GWL. During this period the reduced precipitation and soil moisture has a stronger impact on the evapotranspiration amounts than the increasing temperature. On average, the simulations project a small net increase of annual evapotranspiration of 1% for the +2°C GWL, and no net changes under the +3°C GWL.

Overall, the results indicate that the net reduction in precipitation and the resulting decrease in soil moisture are the main drivers for the projected drought trends – whereas changes in evapotranspiration (and thus temperature changes) play only a minor role.

3.2 FUTURE CHANGES IN RECURRENT DROUGHT CHARACTERISTICS

Next, we analyse projected changes in the recurrence of drought events in IP, focusing on both maximum duration and frequency. With this aim, we compare the two future GWLs to the historical reference period (1971–2000; matching a GWL of +0.5°C).

3.2.1 Recurrent dry years

Figure 5 shows the recurrent dry year index (RDYI; top row) and the corresponding number of dry year periods (NDYP; bottom row) for the EURO-CORDEX ensemble mean. For the future GWLs, robust signals with a minimum of 17 ensemble members agreeing on the sign

of change are dotted. In the reference period (*Figure 5a, d*), the ensemble mean simulates only single dry years, i.e. that RDYI is below 2 for all of IP in the ensemble mean. Consequently, no dry year periods with more than two consecutive dry years are identified (NDYP=0). For the +2°C GWL (*Figure 5b, e*), the southernmost region in IP is affected by two or three consecutive dry years, which occur only once in the whole 30-year period (NDYP=1). At the same time, no dry years are identified in the northernmost parts in the ensemble mean. For the rest of IP, only single dry years, and therefore no dry year periods, are projected in the ensemble mean. The spread between the individual ensemble members is large for the +2°C GWL, resulting in mostly non-robust climate change signals. If global warming increases to +3°C (*Figure 5c, f*), the ensemble mean reveals a clear and (in most regions) robust increase in the duration and frequency of recurrent dry years – with a distinct North–South-gradient. For the southern half of IP, RDYI increases to at least 2. Some recurrent events can last four years in the southernmost part (*Figure 5c*). Simultaneously, the frequency of recurrent events is projected to increase – from single dry periods in Central IP (non-robust) up to three dry periods in Southern IP (likely).

3.2.2 Recurrent drought years

The consecutive drought year index based on DI (CDY) and the corresponding number of drought periods (NDP) is illustrated in *Figure 6*. An overview of the variations in CDY (NDP) for all sub-regions is presented in *Table 3* (Supplementary Table S1), displaying the ensemble minima/mean/maxima. For the reference period 1971–2000 (*Figure 6a, d*), all ensemble members show a CDY of either 1 or 2 for IP, resulting in an ensemble mean of 1.32. Accordingly, the number of drought periods ranges between 0 and 1, with an ensemble mean of 0.32.
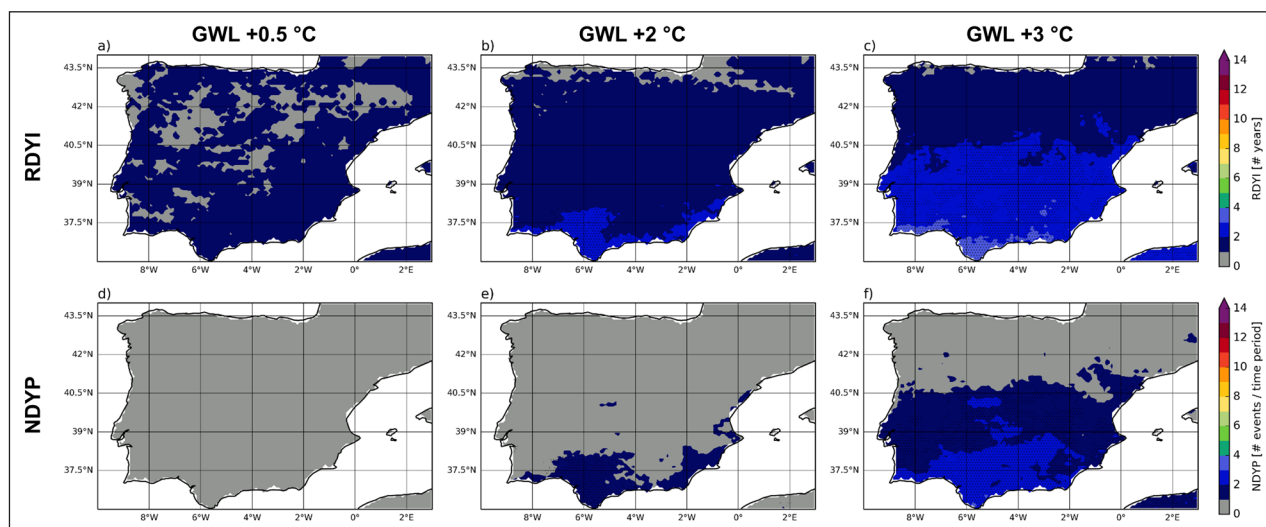
Figure 5 Recurrent dry year index (RDYI; top row) and corresponding number of dry year periods (NDYP; bottom row) derived from the ensemble mean for a GWL of +0.5°C (historical reference; **a**, **d**), +2°C (**b**, **e**), and +3°C (**c**, **f**). For future GWLs, black dots indicate robust climate change signals, meaning that 17 or more ensemble members (corresponds to 68%) agree on the sign of change.
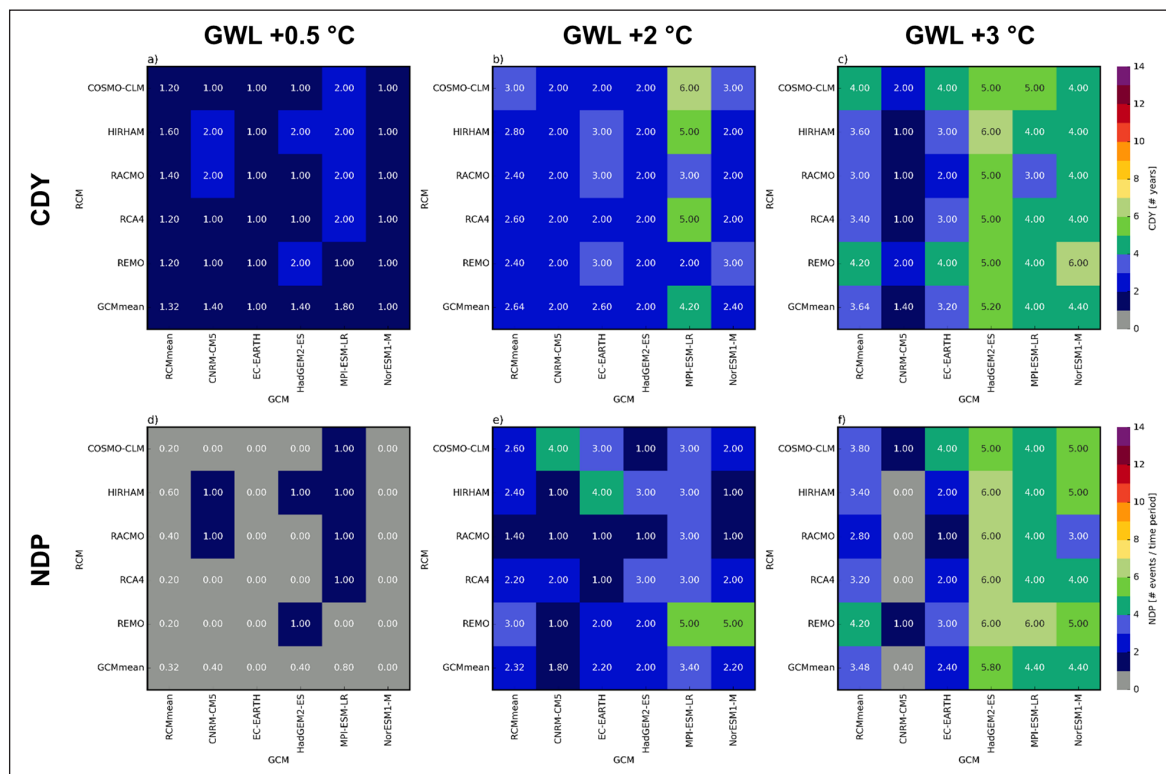
Figure 6 Consecutive drought year index (CDY; top row) and corresponding number of drought periods (NDP; bottom row) for the individual ensemble members derived for whole IP for a GWL of +0.5°C (historical reference; **a**, **d**), +2°C (**b**, **e**), and +3°C (**c**, **f**). For each matrix, rows represent RCMs and columns GCMs, while the RCM (GCM) mean is depicted in the first column (last row).

		CDY			CDY-EDI		
		GWL +0.5°C	GWL +2°C	GWL +3°C	GWL +0.5°C	GWL +2°C	GWL +3°C
IP	min	1.00	2.00	1.00	1.00	2.00	2.00
	mean	1.32	2.64	3.64	1.56	3.48	5.28
	max	2.00	6.00	6.00	3.00	7.00	14.00
IP-NW	min	1.00	1.00	1.00	1.00	1.00	1.00
	mean	1.20	1.68	2.44	1.92	3.32	**5.96**
	max	2.00	3.00	4.00	3.00	7.00	**18.00**
IP-NE	min	1.00	1.00	1.00	1.00	2.00	2.00
	mean	1.12	1.96	2.80	**1.96**	**3.84**	5.52
	max	2.00	5.00	5.00	**4.00**	7.00	14.00
IP-E	min	1.00	1.00	1.00	1.00	1.00	1.00
	mean	1.36	1.88	2.32	1.64	2.52	3.76
	max	3.00	5.00	5.00	3.00	6.00	8.00
IP-SW	min	1.00	2.00	1.00	1.00	1.00	1.00
	mean	1.68	3.12	3.76	1.52	3.24	4.88
	max	**4.00**	6.00	**10.00**	3.00	6.00	10.00
IP-SE	min	1.00	1.00	1.00	1.00	1.00	2.00
	mean	**1.76**	**3.48**	**4.52**	1.48	3.04	5.08
	max	3.00	**9.00**	7.00	3.00	7.00	14.00

Table 3 Consecutive drought year index (CDY; left) and consecutive drought year index based on EDI (CDY-EDI; right) for a GWL of +0.5°C, +2°C, and +3°C. Numbers represent the ensemble minimum, the ensemble mean and the ensemble maximum – derived as spatial average for IP and its five sub-regions. The highest values per GWL are highlighted in bold.

Comparable numbers are found for Northern IP, while both duration and frequency values are slightly higher in Southern IP (see ***Table 3***, and Figures S7 and S8). All simulations driven by EC-EARTH and NorESM1-M feature only single and no recurrent drought events. For the +2°C GWL (***Figure 6b, e***), the ensemble mean CDY increases to 2.64 for IP. Overall, 21 out of 25 ensemble members agree on this positive trend, with values varying between 2 and 6. Lowest CDY numbers are simulated by CNRM-CM5- and HadGEM2-ES-driven runs, while simulations with MPI-ESM-LR show the highest values. At the same time, all GCM-RCM model chains – except two members driven by CNRM-CM5 – project an increase in recurrent drought frequency. The ensemble mean reaches up to 2.32. On the regional scale (***Tables 3*** and S1), trends in both CDY and NDP are strongest (weakest) for IP-SE (IP-NW), which also shows the largest (lowest) ensemble spread. For the +3°C GWL (***Figure 6c, f***), the maximum duration of recurrent drought events increases further for IP and its sub-regions: The ensemble mean CDY reaches a value of 3.64 in IP, and up to five consecutive years in IP-SE. Additionally, the ensemble spread further increases, with numbers ranging from 1 to 7 for IP. Again, lowest CDY are found for CNRM-CM5-driven simulations, while the strongest increase is simulated by members forced with HadGEM2-ES and NorESM1-M. Nearly all ensemble members project an increasing frequency with values between 1 and 6. Overall, results based on CDY and NDP

show a robust trend towards longer recurrent drought events. Signals are stronger for a higher level of global warming and depend primarily on the choice of GCM. From the regional perspective, signals typically show a north-south gradient, with lowest values for IP-NW and highest for IP-SE.

The maximum duration and the frequency of recurrent drought events is generally higher for the one-dimensional indices based on spatially averaged EDI (CDY-EDI and NDP-EDI), as shown in ***Figure 7***. Analogous to ***Figure 6***, it presents the results for the individual ensemble members for all three GWLs and whole IP. For 1971–2000 (***Figure 7a, d***), CDY-EDI ranges between 1 and 3 for IP, with an ensemble mean of 1.56. Correspondingly, the ensemble members identify 0 to 2 drought periods, which results in a mean NDP-EDI of 0.72. For the +2°C GWL (***Figure 7b, e***), the ensemble mean CDY-EDI increases to 3.48, while the ensemble members vary between 2 and 7 consecutive drought years. In the CNRM-CM5 sub-ensemble, one member projects a decrease in drought duration and two members show no change. All other model chains agree on the positive trend in CDY-EDI. Regarding recurrent drought frequency, 23 out of 25 ensemble members simulate an increase of NDP-EDI with values between 1 and 6 and an ensemble mean of 3.08. For the +3°C GWL (***Figure 7c, f***), CDY-EDI shows a strong and robust increase in the ensemble mean to 5.28. In addition, the ensemble spread becomes larger
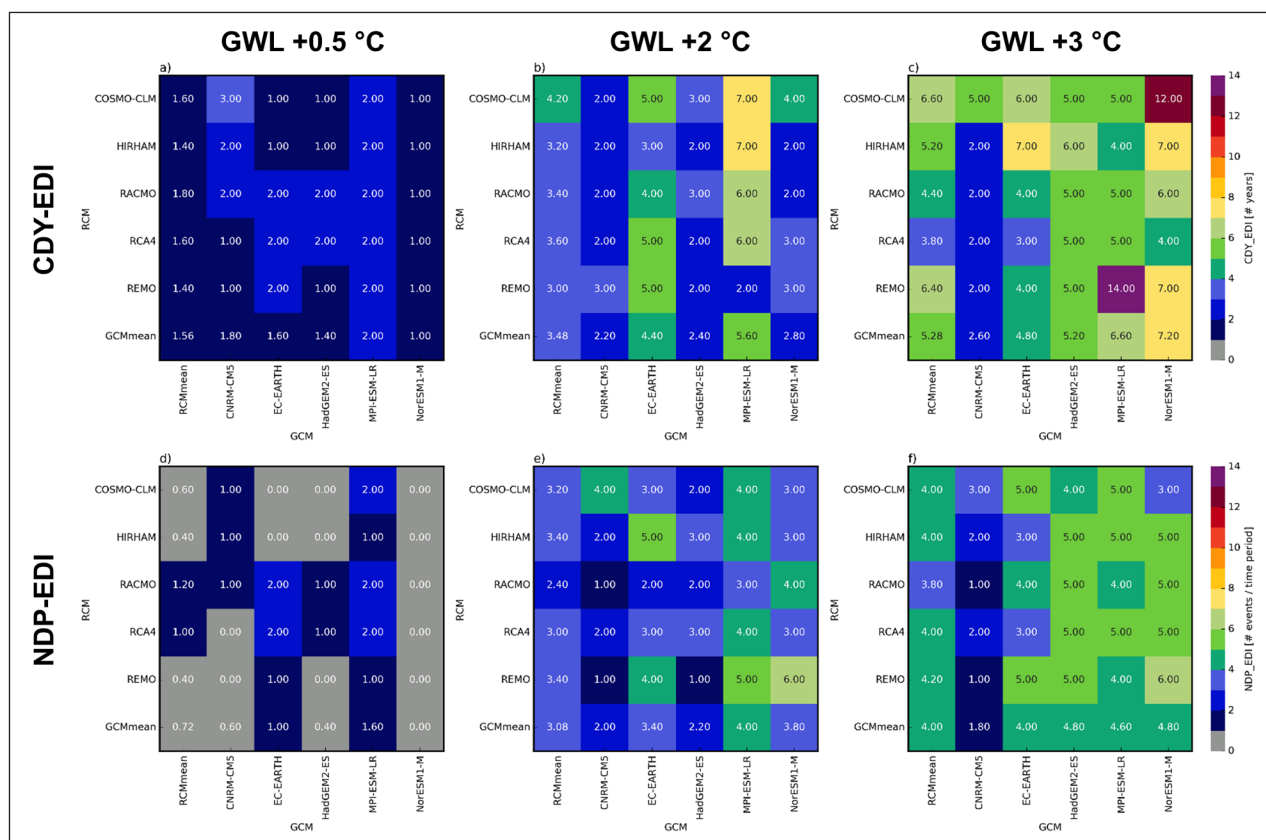
Figure 7 Same as Figure 6, but for consecutive drought year index based on EDI (CDY-EDI; top row) and corresponding number of drought periods (NDP-EDI; bottom row).

with a minimum of 2 and a maximum of 14 consecutive drought years (in the 30-year period). The strongest increase is projected by the NorESM-1-M sub-ensemble, while smallest changes can again be found for CNRM-CM5. Relative to the reference period, 23 of 25 ensemble members agree on the positive trend. However, when comparing the +2°C and the +3°C GWL, some runs (especially those driven by MPI-ESM-LR) show a negative trend. Except of CNRM-CM5, all models simulate a further increase in NDP-EDI for the +3°C GWL. The ensemble mean reaches 4.0, while the individual ensemble members range between 1 and 6. The stationary or even decreasing trend for CNRM-CM5 is striking. On the whole, the one-dimensional CDY-EDI and NDP-EDI indicate a strong and likely increase in the duration of recurrent drought events. Again, climate change signals show a slightly bigger spread regarding the choice of GCMs than RCMs. Contrary to CDY (NDP), the different sub-regions (*Tables 3* and S1, as well as Figures S9 and S10) show similar trends compared to whole IP for CDY-EDI (NDP-EDI). Moreover, the projected trends are usually larger for EDI than for indices based on DI. This could hint at a higher climate sensitivity in EDI compared to DI.

Figure 8 presents a grid point-wise view of CDY-EDI (top) and NDP-EDI (bottom) for the multi-model ensemble mean. In the historical period (*Figure 8a, d*), the ensemble mean simulates only single drought events for Southern and large parts of Central IP (CDY-EDI < 2). In Northern IP, recurrent events last for two or three years. Consequently, single drought periods are identified for this region, while no drought periods are found for Southern and Central IP (NDP-EDI=0). For the +2°C GWL (*Figure 8b, e*), the ensemble mean projects an overall robust increase in the duration of drought events to two to four years for all of IP. At single grid points, drought events can persist for five years. Additionally, a higher

frequency of recurrent droughts is likely for large parts of IP. The ensemble mean projection reveals two to three drought periods under a global warming of +2°C. Trends in CDY-EDI and NDP-EDI are even stronger and more robust for the +3°C GWL (*Figure 8c*, *f*). The duration of recurrent events is clearly increasing to values between 5 and 10 in the ensemble mean. Thereby, the spatial pattern seems to follow the Iberian topography with higher numbers in higher elevations. The number of drought periods is likewise increasing and ranges from 3 to 5. The lower NDP-EDI values in mountainous regions correspond well to the higher CDY-EDI in the same area (see also Section 2.4).

Overall, our results reveal a clear increase in the duration and frequency of recurrent events on the Iberian Peninsula in future climate scenarios. The climate change signals suggest an acceleration of trends with time, as the difference between the reference period and the +2°C GWL is usually smaller than the one between the two future GWLs. The projected changes depend on the applied index. Typically, trends are lower and less robust for RDYI (NDYP) and CDY (NDP), and higher and more likely for CDY-EDI (NDP-EDI). In addition, the magnitude of climate change signals can vary strongly across the individual ensemble members. Among the GCMs, CNRM-CM5 (NorESM1-M) generally shows the weakest (strongest) trends, while it is RACMO (COSMO-CLM) on the regional scale.

4. SUMMARY AND DISCUSSION

In this study, we investigated potential climate change impacts on the recurrence of drought events in the Iberian Peninsula. With this aim, we applied the new set of indices developed by Moemken and Pinto (2022) to a
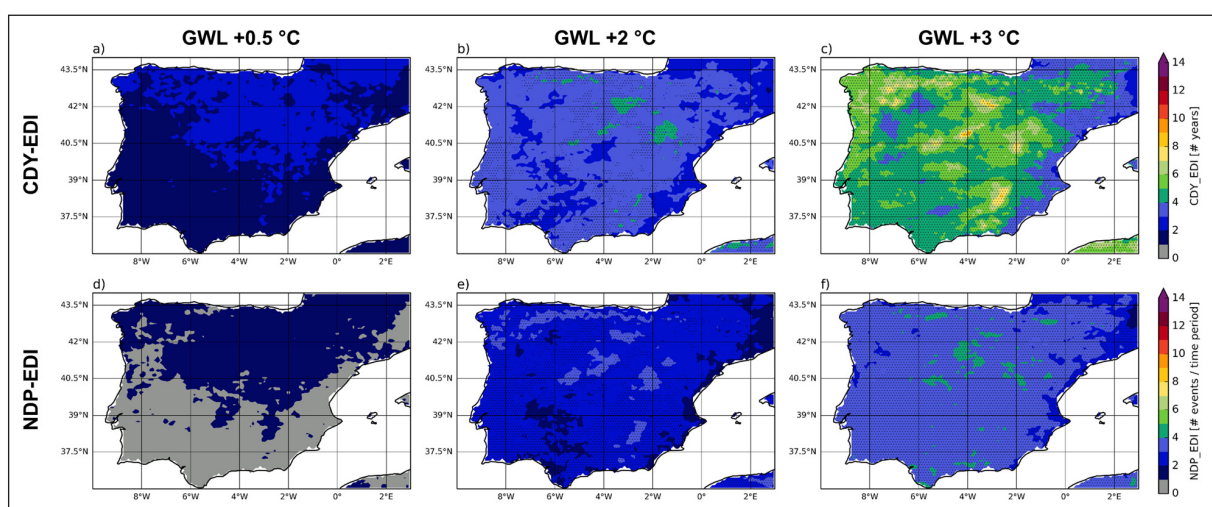
Figure 8 Consecutive drought year index based on EDI (CDY-EDI; top row) and corresponding number of drought periods (NDP-EDI; bottom row) derived from the ensemble mean for a GWL of +0.5°C (historical reference; **a**, **d**), +2°C (**b**, **e**), and +3°C (**c**, **f**). For future GWLs, black dots indicate robust climate change signals, meaning that 17 or more ensemble members (corresponds to 68%) agree on the sign of change.

large EURO-CORDEX GCM-RCM ensemble. Precipitation was bias-adjusted using a simple multiplicative approach. Climate change signals were estimated using the RCP8.5 scenario for two global warming levels relative to pre-industrial climate conditions: +2°C and +3°C. The main results can be summarized as follows:

- The ensemble mean projections reveal a general tendency towards negative EDI values and thus more severe drought conditions for most of IP under future global warming – caused by an overall decrease in precipitation and soil water content, and a slightly increased net evapotranspiration. Changes are mostly robust (in the sense that at least 68% of the ensemble members agree on the sign of change) and more pronounced under the higher GWL of +3°C.
- The duration of recurrent drought events is projected to significantly increase under future climate conditions. The climate change signals are robust for most of IP in a +2°C and for all of IP in a +3°C warmer world. Should global warming exceed a +3°C threshold, the majority of models agrees on an almost permanent state of drought – with normal (according to present day conditions) or even wet years becoming rare events.
- Regarding the frequency of recurrent events, an overall increase is identified, with exception of models (e.g. HadGEM2-ES) and regions (IP-SE) with the strongest drying trend. Here, a decrease in recurrent drought frequency is projected.
- The magnitude of climate change signals shows some sensitivity regarding the choice of index. Indices based on EDI seem to have a higher sensitivity to climate change, resulting in even longer and more frequent recurrent drought events.
- The future projections reveal some uncertainty in the magnitude of change, which varies across the individual GCM-RCM model chains. In agreement with studies like Räisänen (2007), GCMs contribute more to this uncertainty than RCMs. Nevertheless, most ensemble members agree on the sign of change, particularly for the end of the century.

Various studies investigated potential impacts of climate change on drought occurrence in Europe – and specifically the Mediterranean region – in recent years (e.g. Stagge et al., 2015; Guerreiro et al., 2017; Spinoni et al., 2018; 2020). Although based on different datasets and a variety of indices for the identification of drought events, all studies agree on an increase in the severity and frequency of droughts over Iberia under future climate conditions. As a result, the positive drought trend of recent decades (Coll et al., 2017; Páscoa et al., 2017; Spinoni et al., 2017) appears to be continuing and intensifying towards the end of the 21st century (Spinoni et al., 2018). Our study is the first to explicitly focus on the recurrence of these

drought events, i.e. the occurrence of individual droughts in consecutive years, thereby extending the findings from the aforementioned studies. Our results fit well to their conclusions, as an increase in drought duration and/or frequency also enhances the probability of events occurring in successive years. This is clearly shown in our study, where climate projections reveal an increase in the duration and frequency of recurrent events.

Our study is based on a single high-emission, non-mitigation scenario – RCP8.5. For this scenario, data availability is largest in EURO-CORDEX. However, projected changes depend strongly on the choice of emission scenario and the consideration of a second, more moderate, scenario, would thus allow a better quantification of uncertainties in these changes. In order to address this issue, we decided to analyse climate change signals for different global warming levels with respect to pre-industrial conditions instead of using fixed time slices (as e.g. done in Spinoni et al., 2018; 2020). According to IPCC (2021), regional climate impacts relate nearly linearly to changes in global temperature and are often independent of the emission scenario for a given level of global warming. This fits well to previous studies like Spinoni et al. (2018), who reveal an increase in drought frequency and severity already under the moderate RCP4.5 scenario. On this basis, we can assume a likewise increase in recurrent drought duration and frequency in more moderate emissions scenarios. Nevertheless, future studies should also include more moderate scenarios and the new Shared Socioeconomic Pathways (SSPs) of CMIP6 (Eyring et al., 2016). This would allow to assess a broader range of possible future pathways.

In accordance with previous studies (e.g. Liang et al, 2008; Ehret et al., 2012), first results point at a distinct positive bias of model precipitation compared to E-OBS. A simple multiplicative bias adjustment (Berg et al., 2012) is applied to reduce the mean bias and to increase the representativeness of the annual cycle. Furthermore, a bias adjustment ensures the comparability of the different GCM-RCM chains. After the bias correction, both the spatial distribution and the annual cycle of precipitation is well represented in the EURO-CORDEX ensemble. Only small differences in the ensemble mean remain over parts of IP.

After the bias adjustment, the chosen multi-model ensemble seems suitable to evaluate recurrent drought characteristics in climate projections, in particular regarding the ensemble mean. Results for the historical reference period (1971–2000) are consistent with those by Moemken and Pinto (2022) for various observational and reanalysis datasets for 1981–2015. Both studies show that the number of identified recurrent drought events generally depends on the index – with lowest numbers for RDYI and highest values for CDY-EDI. Additionally, Moemken and Pinto (2022) found some sensitivity regarding the choice of dataset, both in terms

of magnitude as well as in terms of affected region. In general, an enhanced number of dry/drought events is identified in datasets with higher spatial resolution (e.g. E-OBS with 0.1° resolution vs ERA5 with 0.25° resolution). In both studies, the maximum duration and the frequency of recurrent events are in the same order of magnitude and the spatial patterns match to a large extent. Differences seem to result mostly from the different time periods (1971–2000 vs 1981–2015) and the smoothing in the EURO-CORDEX ensemble mean. Furthermore, both studies agree on a higher sensitivity of EDI-based indices regarding the identification and characterisation of (recurrent) drought events. As already discussed in Moemken and Pinto (2022), one possible reason for this higher sensitivity could be the 'memory effect' of EDI. By including the weighted precipitation of the last 365 days, EDI may be less influenced by inter-seasonal and inter-annual variability. Another reason could be that EDI is a 2D index, thereby reacting stronger to regional-to-local changes than the one-dimensional DI. Moreover, the chosen threshold for the identification of drought years (90 EDI dry days per year), which proved suitable for the present climate, could probably be too low under (drier) future climate conditions. This would result in an overestimation of single drought events and thus of recurrent drought characteristics in future climate projections.

In this study, we gave EDI preference over the more widely used Standardized Precipitation Index (SPI; McKee et al., 1993). This choice was motivated by several previous studies. The main difference between EDI and SPI is the implementation of daily compared to monthly precipitation data in the calculation. By using daily data, EDI takes into account the aggravating effects of runoff and evapotranspiration, which can build up over time – whereas commonly used indices like SPI fail to do so (Byun and Wilhite, 1999). This might be an advantage of EDI over SPI for ecosystem impact studies. In addition, Kim and Byun (2009) found that monthly indices in climate change studies are unable to consider the effect of enhanced precipitation variability. An increase in precipitation variability under future climate conditions indicates that the precipitation frequency is decreasing while the precipitation intensity is simultaneously increasing. This would result in a higher number of days with little-to-no precipitation, which is not captured by indices based on monthly or annual time scales. Finally, Moemken and Pinto (2022) compared EDI and SPI for both single and recurrent drought events. They could show that results for EDI and SPI match well for the current climate, especially for SPI-12. In particular, the 'memory effect' of EDI seems to relate well to the multi-scalar character of SPI.

In our study, we only focus on precipitation-based drought indicators – due to several reasons: For one, we needed indices that are easily applicable to a large multi-

model ensemble of high-resolution regional climate simulations (e.g. Jacob et al., 2014; Berg et al., 2019). Indices derived from multiple variables would inevitably limit the data availability and lead to higher computing and processing times. Moreover, the calculation of 'multi-variate' drought indices (like SPEI (Standardized Precipitation Evapotranspiration Index; Vicente-Serrano et al., 2010) or PDSI (Palmer Drought Severity Index; Palmer, 1965)) from climate model data would require a multi-variate but physically consistent bias-correction approach, which would further increase the complexity of the task. Beyond that, 'multi-variate' indices like SPEI and PDSI depend strongly on the parameterisation of evapotranspiration. Studies like Milly and Dunne (2017) could show that future trends of parameterised evapotranspiration are often overestimated in climate change simulations. This would also influence the reliability of climate change signals of the corresponding drought indicators. Nevertheless, we additionally analysed the mean annual cycle and the future changes of several key variables for drought behaviour in IP provided by the RCM ensemble – namely temperature, precipitation, soil moisture and evapotranspiration. The results demonstrate that the net reduction of precipitation leads to drier soil, thereby confirming the increasing drought tendency deduced by the indices. This trend is more pronounced for the +3°C warming level compared to the +2°C GWL. The net contribution of evapotranspiration is almost negligible, with a slight increase from autumn to spring and a reduction in summer. Thus, precipitation deficits are the main driver for the projected trends in (recurrent) drought events as the temperature changes are almost homogeneous throughout the year.

As the Iberian Peninsula is prone to drought events (Hoerling et al., 2012; Seneviratne et al., 2012; Coll et al., 2017) and water scarcity (Iglesias et al., 2009) already under present day climate conditions, an increase in drought severity and frequency with ongoing climate change will further exacerbate this threat and may lead to an increased competition of different water using sectors (Blauhut et al., 2015; Caldeira et al., 2015; Naumann et al., 2015; Haberstroh et al., 2021). Longer-lasting and more frequent recurrent drought events – as identified in this study – could prove particularly hazardous, as they further reduce the available/required recovery time and thus may lead to a critical destabilization.

Overall, our study presents novel insights in the recurrence of drought events in the Iberian Peninsula under future climate conditions. We show that IP faces a drastic increase in the risk of both longer and more frequent recurrent drought events with ongoing climate change. Should we fail to keep global warming well below +3°C (better below +2°C), a majority of models agrees on an almost permanent state of drought – with severe consequences for all water-dependent sectors in Iberia.

Our results could support stakeholders and decision makers in developing and implementing mitigation and adaptation strategies to secure water supply in future decades.

DATA ACCESSIBILITY STATEMENT

The input data for this study are freely available from:

- *https://www.ecad.eu/download/ensembles/download.php* (E-OBS)
- *https://esgf-data.dkrz.de/search/cordex-dkrz/* (EURO-CORDEX)

The processed data that support the findings of this study are available from the corresponding author upon reasonable request.

ADDITIONAL FILE

The additional file for this article can be found as follows:

- **Supporting Information.** Figures S1–S10 and Table S1. DOI: *https://doi.org/10.16993/tellusa.52.s1*

ACKNOWLEDGEMENTS

COMPETING INTERESTS

The authors have no competing interests to declare.

AUTHOR CONTRIBUTIONS

JM and JGP conceived and designed the study. JM wrote the initial paper draft. BK and JM performed the data analysis. BK, FE and HF developed the bias correction. All authors discussed the results and contributed with manuscript revisions.

AUTHOR AFFILIATIONS

Julia Moemken (iD) *orcid.org/0000-0002-9432-0202*
Institute of Meteorology and Climate Research (IMK-TRO), Karlsruhe Institute of Technology (KIT), Karlsruhe, Germany

Benjamin Koerner
Institute of Meteorology and Climate Research (IMK-TRO), Karlsruhe Institute of Technology (KIT), Karlsruhe, Germany; Now at: Institute of Physics and Meteorology, University of Hohenheim, Hohenheim, Germany

Florian Ehmele (iD) *orcid.org/0000-0003-4230-9295*
Institute of Meteorology and Climate Research (IMK-TRO), Karlsruhe Institute of Technology (KIT), Karlsruhe, Germany

Hendrik Feldmann (iD) *orcid.org/0000-0001-6987-7351*
Institute of Meteorology and Climate Research (IMK-TRO), Karlsruhe Institute of Technology (KIT), Karlsruhe, Germany

Joaquim G. Pinto (iD) *orcid.org/0000-0002-8865-1769*
Institute of Meteorology and Climate Research (IMK-TRO), Karlsruhe Institute of Technology (KIT), Karlsruhe, Germany

REFERENCES

Barriopedro, D, Fischer, EM, Luterbacher, J, Trigo, RM and **Garcia-Herrera, R.** 2011. The Hot Summer of 2010: Redrawing the Temperature Record Map of Europe. *Science*, 322: 220–224. DOI: *https://doi.org/10.1126/science.1201224*

Bentsen, M, et al. 2013. The Norwegian Earth System Model, NorESM1-M – Part 1: Description and basic evaluation of the physical climate. *Geosci Model Dev.*, 6: 687–720. DOI: *https://doi.org/10.5194/gmd-6-687-2013*

Berg, P, Christensen, OB, Klehmet, K, Lenderink, G, Olsson, J, Teichmann, C and **Yang, W** 2019. Summertime precipitation extremes in a EURO-CORDEX 0.11° ensemble at an hourly resolution. *Nat. Hazards Earth Syst. Sci.*, 19: 957–971. DOI: *https://doi.org/10.5194/nhess-19-957-2019*

Berg, P, Feldmann, H and **Panitz, H-J** 2012. Bias correction of high resolution regional climate model data. *J. Hydrol.*, 448: 80–92. DOI: *https://doi.org/10.1016/j.jhydrol.2012.04.026*

Blauhut, V, Gudmundsson, L and **Stahl, K.** 2015. Towards pan-European drought risk maps: quantifying the link between

drought indices and reported drought impacts. *Environ. Res. Lett.*, 10: 014008. DOI: *https://doi.org/10.1088/1748-9326/10/1/014008*

Byun, H-R and **Wilhite, DA.** 1999. Objective Quantification of Drought Severity and Duration. *J. Climate*, 12: 2747–2756. DOI: *https://doi.org/10.1175/1520-0442(1999)012<2747:OQODSA>2.0.CO;2*

Caldeira, MC, Lecomte, X, David, TS, Pinto, JG, Bugalho, MN and **Werner, C.** 2015. Synergy of extreme drought and shrub invasion reduce ecosystem functioning and resilience in water-limited climates. *Sci. Rep.*, 5: 15110. DOI: *https://doi.org/10.1038/srep15110*

Cardell, MF, Romero, R, Amengual, A, Homar, V and **Ramis, C.** 2019. A quantile-quantile adjustment of the EURO-CORDEX projections for temperatures and precipitation. *Int. J. Climatol.*, 39: 2901–2918. DOI: *https://doi.org/10.1002/joc.5991*

Christensen, OB, Christensen, JH, Machenhauer, B and **Botzet, M.** 1998. Very high-resolution regional climate simulations over Scandinavia – Present climate. *J Climate*, 11: 3204–3229. DOI: *https://doi.org/10.1175/1520-0442(1998)011<3204:VHRRCS>2.0.CO;2*

Christensen, JH and **Christensen, OB.** 2007. A summary of the PRUDENCE model projections of changes in European climate by the end of this century. *Clim. Change*, 81: 7–30. DOI: *https://doi.org/10.1007/s10584-006-9210-7*

Ciais, PH, et al. 2005. Europe-wide reduction in primary productivity caused by the heat and drought in 2003. *Nature*, 437: 529–533. DOI: *https://doi.org/10.1038/nature03972*

Coll, JR, Aguilar, E and **Ashcroft, L.** 2017. Drought variability and change across the Iberian Peninsula. *Theor. Appl. Climatol.*, 130: 901–916. DOI: *https://doi.org/10.1007/s00704-016-1926-3*

Collins, WJ, et al. 2011. Development and evaluation of an Earth-System model – HadGEM2. *Geosci Model Dev*, 4: 1051–1075. DOI: *https://doi.org/10.5194/gmd-4-1051-2011*

Cook, BI, Ault, TR and **Smerdon, JE.** 2015. Unprecedented 21st century drought risk in the American Southwest and Central Plains. *Science Advances*, 1: e1400082. DOI: *https://doi.org/10.1126/sciadv.1400082*

Cornes, R, van der Schrier, G, van den Besselaar, EJM and **Jones, PD.** 2018. An Ensemble Version of the E-OBS Temperature and Precipitation Datasets. *J. Geophys. Res. Atmos*, 123: 9391–9409. DOI: *https://doi.org/10.1029/2017JD028200*

Dai, A. 2011. Drought under global warming: a review. *WIREs Clim. Change*, 2: 45–65. DOI: *https://doi.org/10.1002/wcc.81*

Dai, A. 2013. Increasing drought under global warming in observations and models. *Nature Clim. Change*, 3: 52–58. DOI: *https://doi.org/10.1038/nclimate1633*

Deo, RC, Byun, H-R, Adamowski, JF and **Begum, K.** 2017. Application of effective drought index for quantification of meteorological drought events: a case study in Australia.

Theor. Appl. Climatol., 128: 359–379. DOI: *https://doi.org/10.1007/s00704-015-1706-5*

Ehmele, F, Kautz, L-A, Feldmann, H and **Pinto, JG.** 2020. Long-term variance of heavy precipitation across central Europe using a large ensemble of regional climate model simulations. *Earth Syst. Dynam.*, 11: 469–490. DOI: *https://doi.org/10.5194/esd-11-469-2020*

Ehmele, F, et al. 2022. Adaptation and application of the large LAERTES-EU regional climate model ensemble for modeling hydrological extremes: A pilot study for the Rhine basin. *Nat. Hazards Earth Syst. Sci.*, 22: 677–692. DOI: *https://doi.org/10.5194/nhess-22-677-2022*

Ehret, U, Zehe, E, Wulfmeyer, V, Warrach-Sagi, K and **Liebert, J.** 2012. HESS Opinions "Should we apply bias correction to global and regional climate model data?". *Hydrol. Earth Syst. Sci.*, 16: 3391–3404. DOI: *https://doi.org/10.5194/hess-16-3391-2012*

Esteban-Parra, MJ, Rodrigo, FS and **Castro-Díez, Y.** 1998. Spatial and temporal patterns of precipitation in Spain for the period 1880–1992. *Int. J. Climatol.*, 18: 1557–1574. DOI: *https://doi.org/10.1002/(SICI)1097-0088(19981130)18:14<1557::AID-JOC328>3.0.CO;2-J*

Eyring, V, Bony, S, Meehl, GA, Senior, CA, Stevens, B, Stouffer, RJ and **Taylor, KE.** 2016. Overview of the Coupled Model Intercomparison Project Phase 6 (CMIP6) experimental design and organization. *Geosci. Model Dev.*, 9: 1937–1958. DOI: *https://doi.org/10.5194/gmd-9-1937-2016*

Fang, G, Yang, J, Chen, Y and **Zammit, C.** 2015. Comparing bias correction methods in downscaling meteorological variables for a hydrologic impact study in an arid area in China. *Hydrol. Earth Syst. Sci.*, 19: 2547–2559. DOI: *https://doi.org/10.5194/hess-19-2547-2015*

Feldmann, H, Früh, B, Schädler, G, Panitz, H-J, Keuler, K, Jacob, D and **Lorenz, P.** 2008. Evaluation of the precipitation for South-western Germany from high resolution simulations with regional climate models. *Meteorol. Z.*, 17: 455–465. DOI: *https://doi.org/10.1127/0941-2948/2008/0295*

Forzieri, G, et al. 2016. Multi-hazard assessment in Europe under climate change. *Climatic Change,* 137: 105–119. DOI: *https://doi.org/10.1007/s10584-016-1661-x*

Friedlingstein, P, et al. 2019. Global Carbon Budget 2019. *Earth Syst Sci Data*, 11: 1783–1838. DOI: *https://doi.org/10.5194/essd-11-1783-2019*

Giorgetta, MA, et al. 2013. Climate and carbon cycle changes from 1850 to 2100 in MPI-ESM simulations for the Coupled Model Intercomparison Project phase 5. *J Adv Model Earth Syst.*, 5: 572–597. DOI: *https://doi.org/10.1002/jame.20038*

Giorgi, F, Jones, C and **Asrar, GR.** 2009. Addressing climate information needs at the regional level: The CORDEX framework. *Bulletin – World Meteorological Organization*, 58: 175–183.

Guerreiro, SB, Kilsby, C and **Fowler, HJ.** 2017. Assessing the threat of future megadrought in Iberia. *Int. J. Climatol*, 37: 5024–5034. DOI: *https://doi.org/10.1002/joc.5140*

Haberstroh, S, Caldeira, MC, Lobo-do-Vale, R, Martins, JI, Moemken, J, Pinto, JG and **Werner, C.** 2021. Non-linear plant-plant interactions modulate impact of extreme drought and recovery on a Mediterranean ecosystem. *New Phytol.*, 231: 1784–1797. DOI: *https://doi.org/10.1111/nph.17522*

Haylock, MR, Hofstra, N, Klein Tank, AMG, Klok, EJ, Jones, PD and **New, M.** 2008. A European daily high-resolution gridded data set of surface temperature and precipitation for 1950–2016. *J. Geophys. Res. Atmos.*, 113: D20119. DOI: *https://doi.org/10.1029/2008JD010201*

Herrera, S, Fernández, J and **Gutiérrez, JM.** 2016. Update of the Spain02 gridded observational dataset for EURO-CORDEX evaluation: assessing the effect of the interpolation methodology. *Int. J. Climatol.*, 36: 900–908. DOI: *https://doi.org/10.1002/joc.4391*

Hertig, E. 2004. Assessment of Mediterranean precipitation and temperature under increased greenhouse warming conditions. Dissertation, University of Würzburg (in German), urn:ubn:de:bvb:20-opus-8740.

Hirschi, M, Seneviratne, SI, Alexandrov, V, Boberg, F, Boroneant, C, Christensen, OB, Formayer, H, Orlowsky, B and **Stepanek, P.** 2011. Observational evidence for soil-moisture impact on hot extremes in southeastern Europe. *Nature Geosci.*, 4: 17–21. DOI: *https://doi.org/10.1038/ngeo1032*

Hoerling, M, Eischeid, J, Perlwitz, J, Quan, X, Zhang, T and **Pegion, P.** 2012. On the increased frequency in Mediterranean Drought. *J. Climate*, 25: 2146–2161. DOI: *https://doi.org/10.1175/JCLI-D-11-00296.1*

Iglesias, A, Garrote, L and **Martín-Carrasco, F.** 2009. Drought risk management in Mediterranean river basins. *Integr. Environ. Assess. Manag.*, 5: 11–16. DOI: *https://doi.org/10.1897/IEAM_2008-044.1*

IPCC. 2021. Climate Change 2021: The Physical Science Basis. Contribution of Working Group I to the Sixth Assessment Report of the Intergovernmental Panel on Climate Change. Masson-Delmotte, V, Zhai, P, Pirani, A, Connors, SL, Péan, C, Berger, S, Caud, N, Chen, Y, Goldfarb, L, Gomis, MI, Huang, M, Leitzell, K, Lonnoy, E, Matthews, JBR, Maycock, TK, Waterfield, T, Yelekçi, O, Yu, R and Zhou, B (eds.). Cambridge University Press. In Press

Jacob, D, et al. 2012. Assessing the transferability of the regional climate model REMO to different coordinated regional climate downscaling experiment (CORDEX) regions. *Atmosphere*, 3: 181–199. DOI: *https://doi.org/10.3390/atmos3010181*

Jacob, D, et al. 2014. EURO-CORDEX: New high-resolution climate change projections for European impact research. *Reg. Environ. Change*, 14: 563–578. DOI: *https://doi.org/10.1007/s10113-013-0499-2*

Kamruzzaman, M, Jang, M-W, Cho, J and **Hwang, S.** 2019. Future Changes in Precipitation and Drought Characteristics over Bangladesh under CMIP5 Climatological Projections. *Water*, 11: 2219. DOI: *https://doi.org/10.3390/w11112219*

Khodayar, S, Sehlinger, A, Feldmann, H and **Kottmeier, CH.** 2015. Sensitivity of soil moisture initialization for decadal predictions under different regional climatic conditions in Europe. *Int. J. Climatol*, 35: 1899–1915. DOI: *https://doi.org/10.1002/joc.4096*

Kim, D-W and **Byun, H-R.** 2009. Future pattern of Asian drought under global warming scenario. *Theor. Appl. Climatol*, 98: 137–150. DOI: *https://doi.org/10.1007/s00704-008-0100-y*

Lee, B-R, Oh, S-B and **Byun, H-R.** 2015. The characteristics of drought occurrence in North Korea and its comparison with drought in South Korea. *Theor. Appl. Climatol*, 121: 199–209. DOI: *https://doi.org/10.1007/s00704-014-1230-z*

Liang, X-Z, Kunkel, KE, Meehl, GA, Jones, RG and **Wang, JXL.** 2008. Regional climate models downscaling analysis of general circulation models present climate biases propagation into future change projections. *Geophys. Res. Lett.*, 35: L08709. DOI: *https://doi.org/10.1029/2007GL032849*

Maheras, P, Xoplaki, E and **Kutiel, H.** 1999. Wet and Dry Monthly Anomalies Across the Mediterranean Basin and their Relationship with Circulation, 1860–1990. *Theor. Appl. Climatol.*, 64: 189–199. DOI: *https://doi.org/10.1007/s007040050122*

Maraun, D. 2016. Bias correcting climate change simulations – a critical review. *Curr. Clim. Change Rep.*, 2: 211–220. DOI: *https://doi.org/10.1007/s40641-016-0050-x*

McKee, TB, Doesken, NJ and **Kleist, J.** 1993. The relationship of drought frequency and duration on timescales. *Proceedings of the Eighth Conference on Applied Climatology*, 17–22 January 1993, Anaheim, CA.

Meijgaard, E van, Van Ulft, LH, Lenderink, G, de Roode, SR, Wipfler, L, Boers, R and **Timmermans, RMA.** 2012. Refinement and application of a regional atmospheric model for climate scenario calculations of Western Europe. Climate changes Spatial Planning publication: KvR 054/12, ISBN/EAN 978-90-8815-046-3. pp 44.

Meinshausen, M, et al. 2011. The RCP greenhouse gas concentrations and their extensions from 1765 to 2300. *Climatic Change*, 109: 213–241. DOI: *https://doi.org/10.1007/s10584-011-0156-z*

Milly, PCD and **Dunne, KA.** 2017. A Hydrologic Drying Bias in Water-Resource Impact Analyses of Anthropogenic Climate Change. *J. Am. Water Resour. As.*, 53: 822–838. DOI: *https://doi.org/10.1111/1752-1688.12538*

Min, E, Hazeleger, W, Van Oldenborgh, G and **Sterl, A.** 2013. Evaluation of trends in high temperature extremes in north-western Europe in regional climate models. *Environ. Res. Lett.*, 8: 014 011. DOI: *https://doi.org/10.1088/1748-9326/8/1/014011*

Mishra, AK and **Singh, VP.** 2010. A review of drought concepts. *J. Hydrol.*, 391: 202–216. DOI: *https://doi.org/10.1016/j.jhydrol.2010.07.012*

Moemken, J and **Pinto, JG.** 2022. Recurrence of Drought Events Over Iberia. Part I: Methodology and Application for Present Climate Conditions. *Tellus A,* 74: 222–235. DOI: *https://doi.org/10.16993/tellusa.50*

Naumann, G, Spinoni, J, Vogt, JV and **Barbosa, P.** 2015. Assessment of drought damages and their uncertainties in Europe. *Environ. Res. Lett*., 10: 124013. DOI: *https://doi. org/10.1088/1748-9326/10/12/124013*

Palmer, WC. 1965. Meteorological Droughts. *U.S. Department of Commerce, Weather Bureau Research Paper*, 45: 1–58.

Paredes, D, Trigo, RM, García-Herrera, R and **Trigo, IF.** 2006. Understanding Precipitation Changes in Iberia in Early Spring: Weather Typing and Storm-Tracking Approaches. *J. Hydrometeorol*., 7: 101–113. DOI: *https://doi.org/10.1175/ JHM472.1*

Páscoa, P, Gouveia, CM, Russo, A and **Trigo, RM.** 2017. Drought Trends in the Iberian Peninsula over the Last 112 Years. *Advances in Meteorology*, 4653126. DOI: *https://doi. org/10.1155/2017/4653126*

Peters, GP, Andrew, RM, Boden, T, Canadell, JG, Ciais, P, Le Quéré, C, Marland, G, Raupach, MR and **Wilson, C.** 2013. The challenge to keep global warming below 2°C. *Nature Clim Change*, 3: 4–6. DOI: *https://doi.org/10.1038/ nclimate1783*

Prodhomme, C, Doblas-Reyes, FJ, Bellprat, O and **Dutra, E.** 2016. Impact of land-surface initialization on sub-seasonal to seasonal forecasts over Europe. *Clim. Dyn*., 47: 919–935. DOI: *https://doi.org/10.1007/s00382-015-2879-4*

Räisänen, J 2007. How reliable are climate models? *Tellus A*, 59: 2–29. DOI: *https://doi.org/10.1111/j.1600-0870.2006.00211.x*

Rockel, B, Will, A and **Hense, A.** 2008. Special issue: regional climate modelling with COSMO-CLM (CCLM). *Meteorol Z*, 17: 347–348. DOI: *https://doi.org/10.1127/0941-2948/2008/0309*

Rodriguez-Puebla, C, Encinas, AH, Nieto, S and **Garmendia, J.** 1998. Spatial and temporal patterns of annual precipitation variability over the Iberian Peninsula. *Int. J. Climatol*., 18: 299–316. DOI: *https://doi. org/10.1002/(SICI)1097-0088(19980315)18:3<299::AID-JOC247>3.0.CO;2-L*

Samuelsson, P, Jones, C, Willén, U, Ullerstig, A, Gollvik, S, Hansson, U, Jansson, C, Kjellström, E, Nikulin, G and **Wyser, K.** 2011. The Rossby Centre Regional Climate Model RCA3: model description and performance. *Tellus A*, 63: 4–23. DOI: *https://doi.org/10.1111/j.1600-0870.2010.00478.x*

Santos, JA, Belo-Pereira, M, Fraga, H and **Pinto, JG.** 2016. Understanding climate change projections for precipitation over western Europe with a weather typing approach. *J. Geophys. Res. Atmos*, 121: 1170–1189. DOI: *https://doi. org/10.1002/2015JD024399*

Schwalm, CR, Glendon, S and **Duffy, PB.** 2020. RCP8.5 tracks cumulative CO_2 emissions. *Proc. Natl. Acad. Sci. U.S.A*., 117: 19656–19657. DOI: *https://doi.org/10.1073/ pnas.2007117117*

Seneviratne, SI, et al. 2012. Changes in climate extremes and their impacts on the natural physical environment. In: *Managing the Risks of Extreme Events and Disasters to Advance Climate Change Adaptation,* Field, CB et al.

(eds.). A Special Report of Working Groups I And II of the Intergovernmental Panel on Climate Change (IPCC). Cambridge, UK, and New York, USA: Cambridge University Press, pp. 109–230.

Seneviratne, SI, et al. 2013. Impact of soil moisture-climate feedbacks on CMIP5 projections: First results from the GLACE-CMIP5 experiment. *Geophys. Res. Lett*., 40: 5212–5217. DOI: *https://doi.org/10.1002/grl.50956*

Sheffield, J, Wood, E and **Roderick, M.** 2012. Little change in global drought over the past 60 years. *Nature*, 491: 435–438. DOI: *https://doi.org/10.1038/nature11575*

Spinoni, J, Naumann, G, Vogt, JV and **Barbosa, P.** 2015a. European drought climatologies and trends based on a multi-indicator approach. *Global Planet. Change*, 127: 50–57. DOI: *https://doi.org/10.1016/j. gloplacha.2015.01.012*

Spinoni, J, Naumann, G, Vogt, JV and **Barbosa, P.** 2015b. The biggest drought events in Europe from 1950–2012. *J. Hydrol. Reg. Stud*., 3: 509–524. DOI: *https://doi. org/10.1016/j.ejrh.2015.01.001*

Spinoni, J, Naumann, G and **Vogt, JV.** 2017. Pan-European seasonal trends and recent changes of drought frequency and severity. *Global Planet. Change*, 148: 113–130. DOI: *https://doi.org/10.1016/j.gloplacha.2016.11.013*

Spinoni, J, Vogt, JV, Naumann, G, Barbosa, P and **Dosio, A.** 2018. Will drought events become more frequent and severe in Europe? *Int. J. Climatol*., 38: 1718–1736. DOI: *https://doi.org/10.1002/joc.5291*

Spinoni, J, et al. 2020. Future Global Meteorological Drought Hot Spots: A Study Based on CORDEX Data. *J. Climate*, 33: 3635–3661. DOI: *https://doi.org/10.1175/JCLI-D-19-0084.1*

Stagge, JH, Rizzi, J, Tallaksen, LM and **Stahl, K.** 2015. Future Meteorological Drought: Projections of Regional Climate Models for Europe. *DROUGHT-R&SPI (Fostering European Drought Research and Science-Policy Interfacing) Technical Report No. 25.*

Teichmann, C, Bülow, K, Otto, J, Pfeifer, S, Rechid, D, Sieck, K and **Jacob, D.** 2018. Avoiding Extremes: Benefits of Staying below +1.5°C Compared to +2.0°C and +3.0°C Global Warming. *Atmosphere,* 9: 115. DOI: *https://doi. org/10.3390/atmos9040115*

Touma, D, Ashfaq, M, Nayak, MA, Kao, S-C and **Diffenbaugh, NS.** 2015. A multi-model and multi-index evaluation of drought characteristics in the 21st century. *J. Hydrol*., 526: 196–207. DOI: *https://doi.org/10.1016/j. jhydrol.2014.12.011*

Tramblay, Y, et al. 2020. Challenges for drought assessment in the Mediterranean region under future climate scenarios. *Earth-Sci. Rev*., 210: 103348. DOI: *https://doi.org/10.1016/j. earscirev.2020.103348*

Trenberth, K, Dai, A, van der Schrier, G, Jones, PD, Barichvich, J, Briffa, KR and **Sheffield, J.** 2014. Global warming and changes in drought. *Nature Clim. Change*, 4: 17–22. DOI: *https://doi.org/10.1038/nclimate2067*

Trigo, RM and **DaCamara, CC.** 2000. Circulation weather types and their influence on the precipitation regime in

Portugal. *Int. J. Climatol.*, 20: 1559–1581. DOI: *https://doi.org/10.1002/1097-0088(20001115)20:13<1559::AID-JOC555>3.0.CO;2-5*

Trigo, RM, Pozo-Vázquez, D, Osborn, TJ, Castro-Díez, Y, Gámiz-Fortis, S and **Esteban-Parra, MJ.** 2004. North Atlantic Oscillation influence on precipitation, river flow and water resources in the Iberian Peninsula. *Int. J. Climatol.*, 24: 925–944. DOI: *https://doi.org/10.1002/joc.1048*

Van Engelen, A, Klein Tank, A, van der Schrier, G and **Klok, L.** 2008. European Climate Assessment & Dataset (ECA&D), Report 2008. KNMI, *https://www.ecad.eu//documents/ECAD_report_2008.pdf*.

Vautard, R, Gobiet, A, Sobolowski, S, Kjellström, E, Stegehuis, A, Watkiss, P, Mendlik, T, Landgren, O, Nikulin, G and **Teichmann, C.** 2014. The European climate under a 2°C global warming. *Environ. Res. Lett.*, 9: 034006. DOI: *https://doi.org/10.1088/1748-9326/9/3/034006*

Vicente-Serrano, SM, Beguería, S and **López-Moreno, JI.** 2010. A Multiscalar Drought Index Sensitive to Global Warming: The Standardized Precipitation Evapotranspiration Index. *J. Climate*, 23: 1696–1718. DOI: *https://doi.org/10.1175/2009JCLI2909.1*

Voldoire, A, et al. 2013. The CNRM-CM5.1 global climate model: description and basic evaluation. *Clim. Dyn.*, 40: 2091–2121. DOI: *https://doi.org/10.1007/s00382-011-1259-y*

Wilhite, DA, Svoboda, MD and **Hayes, MJ.** 2007. Understanding the complex impacts of drought: A key to enhancing drought mitigation and preparedness. *Water Resour. Manage*, 21: 763–774. DOI: *https://doi.org/10.1007/s11269-006-9076-5*

WMO. 2006. Drought monitoring and early warning: concepts, progress and future challenges. *WMO-No. 1006*, ISBN: 978-92-63-11006-0

World Economic Forum. 2019. *The Global Risks Report 2019*, 14th Edition. Geneva, Switzerland: World Economic Forum. ISBN: 978-1-944835-15-6.

Yang, X, Wood, EF, Sheffield, J, Ren, L, Zhang, M and **Wang, Y.** 2018. Bias Correction of Historical and Future Simulations of Precipitation and Temperature for China from CMIP5 Models. *J. Hydrometeorol.*, 19: 609–623. DOI: *https://doi.org/10.1175/JHM-D-17-0180.1*

Zhang, X, Alexander, L, Hegerl, GC, Jones, P, Klein, Tank, A, Peterson, TC, Trewin, B and **Zwiers, FW.** 2011. Indices for monitoring changes in extremes based on daily temperature and precipitation data. *WIREs Clim. Change*, 2: 851–870. DOI: *https://doi.org/10.1002/wcc.147*

Zscheischler, J, et al. 2020. A typology of compound weather and climate events. *Nat. Rev. Earth Environ.*, 1: 333–347. DOI: *https://doi.org/10.1038/s43017-020-0060-z*